Proceedings of the 17th World Congress
The International Federation of Automatic Control
Seoul, Korea, July 6-11, 2008

Current Output Observer for Discrete-Time Nonlinear Stochastic Systems

Tongyan Zhai * Edwin E. Yaz Chung Seop Jeong *****

Department of Electrical and Computer Engineering, Marquette University, Milwaukee, WI 53201, USA
Tel: 414-288-6820; E-mail: * tong.zhai@mu.edu, **edwin.yaz@mu.edu, *** chung.jeong@mu.edu

Abstract: A Current Output Observer is presented and its estimation error performance is compared to that of the Extended Kalman Filter. It is shown that performance improvement can be obtained by this new scheme with minor increase in computational load. In order to obtain stronger results, scalar nonlinear stochastic systems are focused on. These systems are categorized based on the derivatives of their nonlinear functions. It is shown that different state estimation performance is achieved when the Current Output Observer is applied to scalar nonlinear systems in these different categories, which allows the convergence property to be known before its implementation. This provides insight into what is going to happen in applications, e.g. for a nonlinear estimator used in chaotic synchronization. Simulation studies involving nonlinear estimation - based chaotic synchronization complement the theory presented.

1. INTRODUCTION

Extended Kalman Filter (EKF) has been well developed and extensively applied in the area of nonlinear state estimation (Anderson and Moore, 1979; Lewis, 1986; Gustafsson, 2000; Kailath, et al., 2000). This extension of the Kalman filter involves successive linearization of the nonlinear dynamics about the current state estimate. It has been proved that this extension of linear optimal estimators is useful and always has bounded estimation error (in a stochastic sense) when the nonlinearities are not severe and noise effects are additive and small (Reif, et al., 1999). This characteristic of EKF provides the motivation for its application to chaotic synchronization in chaotic secure communication systems (Pecora and Carroll, 1990; Sobiski and Thorp, 1998; Cruz and Nijmeijer, 2000; Amirazodi, 2001; Leung and Zhu, 2001; Ruan, et al., 2003a, b; Hounkpevi and Yaz, 2006a, b), which, currently, is our main research interest.

In this work, we present a current output approach to nonlinear stochastic system state estimation, which we call the Current Output Observer (COO). The estimator error performance of COO is shown to be superior to that of EKF. Then, we analyze the scalar case thoroughly to conclude that the steady error variance of COO is determined by whether the upper bound of the derivative of the nonlinear function is greater or less than 1. This theoretical conclusion establishes a simple connection between a characteristic of the nonlinear function in the dynamic system and the performance of its COO as was established in our previous work (Zhai, et al., 2003) for EKF. This provides great convenience in the a-priori analysis of nonlinear state estimation performance and facilitates the design of COO in many applications including chaotic synchronization.

This paper is organized as follows: section 2 presents a derivation of the equations of COO in the n-dimensional case, as well as the derivation of an upper bound on the estimation error variance with respect to the categorization in (Zhai, et al., 2003). Involving an upper bound on the derivative of the nonlinear function in the scalar case. Behavior of COO according to this categorization scheme is discussed. Section 3 gives the Monte-Carlo simulation results for various nonlinear chaotic dynamic systems as the numerical verification of the theoretical ones. Section 4 draws conclusions for this paper regarding the performance of COO.

2. MAIN RESULTS

2.1 Signal Model and Derivation of n-Dimensional COO

Consider the following nth order nonlinear stochastic system with a nonlinear measurement equation:

$$\begin{aligned} x_{n+1} &= f(x_n) + v_n \\ y_n &= h(x_n) + w_n \end{aligned} \tag{2.1}$$

where x_n is the state, x_0 is of mean $\mathrm{E}\{x_0\} = \bar{x}_0$ and covariance P_0, and is uncorrelated with other sources. y_n is the measured output, v_n and w_n are the mutually uncorrelated zero-mean white noises with covariances V and W, respectively. f and h are smooth nonlinearities.

This model can be rewritten in the following form:

$$\begin{aligned} \begin{bmatrix} x_{n+1} \\ x_n \end{bmatrix} &= \begin{bmatrix} f(x_n) \\ x_n \end{bmatrix} + \begin{bmatrix} v_n \\ 0 \end{bmatrix} \\ y_n &= h(x_n) + w_n \end{aligned} \tag{2.2}$$

for use in construction of the COO.

$f(x_n)$ and $h(x_n)$ can be expanded into Taylor series at $\hat{x}_n$ as follows:

$$f(x_n) = f(\hat{x}_n) + A_n(x_n - \hat{x}_n) + H.O.T$$
$$h(x_n) = h(\hat{x}_n) + C_n(x_n - \hat{x}_n) + H.O.T$$

where $A_n = \left.\frac{\partial f}{\partial x}\right|_{x=\hat{x}_n}, C_n = \left.\frac{\partial h}{\partial x}\right|_{x=\hat{x}_n}$. Similar to in EKF, *first order linear approximations for* $f(x_n)$ *and* $h(x_n)$ *are used, so that:*

$$\begin{aligned} f(x_n) &\simeq f(\hat{x}_n) + A_n e_n \\ h(x_n) &\simeq h(\hat{x}_n) + C_n e_n \end{aligned} \tag{2.3}$$

where $e_n = x_n - \hat{x}_n$.

The EKF-based state estimation for the model (2.2) is described as follows:

$$\begin{bmatrix} \hat{x}_{n+1} \\ \hat{x}_n^c \end{bmatrix} = \begin{bmatrix} f(\hat{x}_n) \\ \hat{x}_n \end{bmatrix} + \begin{bmatrix} K_n^1 \\ K_n^2 \end{bmatrix} \left(y_n - h\left(\hat{x}_n \right) \right) \tag{2.4}$$

where $\hat{x}_n^c$ is the current output estimate of $\hat{x}_n$ after receiving the measurement y_n.

When applying the first order linear approximation as (2.3), the estimation error can be evaluated to first order as follows:

$$\begin{aligned} \begin{bmatrix} e_{n+1} \\ e_n^c \end{bmatrix} &= \begin{bmatrix} f(x_n) \\ x_n \end{bmatrix} + \begin{bmatrix} v_n \\ 0 \end{bmatrix} - \begin{bmatrix} f(\hat{x}_n) \\ \hat{x}_n \end{bmatrix} - \begin{bmatrix} K_n^1 \\ K_n^2 \end{bmatrix} \left(y_n - h\left(\hat{x}_n \right) \right) \\ &\simeq \begin{bmatrix} f(\hat{x}_n) + A_n e_n \\ \hat{x}_n \end{bmatrix} + \begin{bmatrix} v_n \\ 0 \end{bmatrix} - \begin{bmatrix} f(\hat{x}_n) \\ \hat{x}_n \end{bmatrix} \\ &- \begin{bmatrix} K_n^1 \\ K_n^2 \end{bmatrix} \left(h(\hat{x}_n) + C_n e_n + w_n - h\left(\hat{x}_n \right) \right) \\ &= \begin{bmatrix} A_n - K_n^1 C_n \\ I - K_n^2 C_n \end{bmatrix} e_n + \begin{bmatrix} I & -K_n^1 \\ 0 & -K_n^2 \end{bmatrix} \begin{bmatrix} v_n \\ w_n \end{bmatrix} \end{aligned} \tag{2.5}$$

The gains K_n^1, K_n^2 are updated at each step as follows:

$$\begin{bmatrix} K_n^1 \\ K_n^2 \end{bmatrix} = \begin{bmatrix} A_n P_n^{11} C_n^T \\ P_n^{11} C_n^T \end{bmatrix} \left(C_n P_n^{11} C_n^T + W \right)^{-1} \tag{2.6}$$

Recall that K_n^1 is the regular EKF gain for the original system (2.1), P_n^{11} is the solution to the Riccati difference equation for the original system (2.1) as well.

Let $P_n = P_n^{11}$ for notational simplicity, so

$$K_n^1 = A_n P_n C_n^T (C_n P_n C_n^T + W)^{-1} \tag{2.7}$$

where

$$P_{n+1} = A_n P_n A_n^T - A_n P_n C_n^T (C_n P_n C_n^T + W)^{-1} C_n P_n A_n^T + V \tag{2.8}$$

For current output observation, the estimation error covariance is

$$\begin{aligned} P_n^c &= E\left\{ e_n^c \left(e_n^c \right)^T \right\} \\ &= \left(I - K_n^2 C_n \right) P_n \left(I - K_n^2 C_n \right)^T + K_n^2 W \left(K_n^2 \right)^T \end{aligned} \tag{2.9}$$

where K_n^2 is the observer gain for the current output estimation, which can be obtained from (2.6).

Substituting from (2.6) into (2.9) yields

$$\begin{aligned} P_n^c &= P_n - P_n C_n^T (C_n P_n C_n^T + W)^{-1} C_n P_n \\ &= (P_n^{-1} + C_n^T W^{-1} C_n)^{-1} \end{aligned} \tag{2.10}$$

where the result is obtained by using the matrix inversion lemma (Horn and Johnson, 1991). Since the subtracted term in (2.10) is positive semi-definite, we have,

$$P_n^c \le P_n \tag{2.11}$$

where this inequality is to be interpreted in terms of the partial (Loewner) ordering of matrices such that $A \le B$ means $B - A$ is a positive semi-definite matrix (Horn and Johnson, 1991).

Equation (2.11) is an important result in that it demonstrates that the linearized estimation error covariance of the COO is bounded above by that of the EKF.

Let us summarize the results:

Theorem 1, For the model (2.1), the COO update equation is given by (2.4) and the gains are given by (2.6), where P_n is the solution to the Riccati difference equation for (2.8), the estimation error covariance of the current output observer is given by (2.10) and is bounded above by that of the EKF as given in (2.11).

Note that the only additional quantity to be computed by the COO is K_n^2 and in implementation, the dimension of the Riccati equation does not change.

2.2 Upper Bound on the Estimation Error Covariance for Scalar systems

Let us consider the first order system model (2.1) with the linear output measurement equation:

$$x_{n+1} = f(x_n)$$
$$y_n = x_n + w_n \tag{2.12}$$

to obtain more concrete results.

This system and measurement scheme is widely used in chaotic synchronization applications (Pecora and Carroll, 1990; Sobiski and Thorp, 1998; Cruz and Nijmeijer, 2000; Amirazodi, 2001; Leung and Zhu, 2001; Ruan, et al., 2003a, b; Hounkpevi and Yaz, 2006a, b).

In this case, EKF gain K_n^1 and P_n are given as,

$$K_n^1 = A_n P_n C_n^T (C_n P_n C_n^T + W)^{-1} = \frac{A_n P_n}{(P_n + W)} \tag{2.13}$$

$$P_{n+1} = A_n^2 P_n - \frac{A_n^2 P_n^2}{(P_n + W)} = \frac{A_n^2 W}{(P_n + W)} P_n \tag{2.14}$$

COO gain K_n^2 and P_n^c are given as

$$K_n^2 = P_n C_n^T \left(C_n P_n C_n^T + W\right)^{-1} = \frac{P_n}{P_n + W} \tag{2.15}$$

$$P_n^c = P_n - \frac{P_n^2}{P_n + W} = \frac{W}{P_n + W} P_n \tag{2.16}$$

Let us assume that there is a ϕ such that $A_n^2 \le \phi < \infty$. An upper bound on estimation error variance for EKF was found to be (Zhai, et al., 2003) :

$$P_n \le \frac{\phi^{n-1}}{\frac{1}{W}\sum_{i=0}^{n-2} \phi^i + \frac{1}{P_0}} \tag{2.17}$$

Similarly, assuming $0 < \Gamma \le A_n^2$. A lower bound on estimation error variance was found to be (Zhai, et al., 2003) :

$$P_n \ge \frac{\Gamma^{n-1}}{\frac{1}{W}\sum_{i=0}^{n-2} \Gamma^i + \frac{1}{P_0}} \tag{2.18}$$

Thus, applying these to our new results in (2.16) for the COO, the following is obtained:

$$P_n^c = \frac{W}{P_n + W} P_n = \frac{1}{\frac{1}{P_n} + \frac{1}{W}} \tag{2.19}$$

$$\limsup_{n\to\infty} P_n^c \le \frac{1}{\frac{1}{\limsup_{n\to\infty} P_n} + \frac{1}{W}} \tag{2.20}$$

Following the analysis results for the EKF in (Zhai, et al., 2003), based on the value of ϕ , we categorize nonlinear systems into three different types:

1) Type I system with $0 < \phi < 1$:

If $0 < \phi < 1$, then (2.17) and (2.20) yield

$$\lim_{n\to\infty} P_n = 0 \tag{2.21}$$

$$\lim_{n\to\infty} P_n^c = 0 \tag{2.22}$$

Note that in this situation, no matter how large the measurement noise variance is, the covariance P_n will go to zero. Moreover, the manner of approach to 0 has a geometric rate. Because $P_n > 0$, from (2.22) the transient values of P_n^c will be smaller than P_n and the value of P_n^c will go to zero in a geometric manner as well.

Type II system with $\phi > 1$:

If $\phi > 1$, then from (2.18)

$$\limsup_{n\to\infty} P_n \le W(\phi - 1) = \overline{P} \tag{2.23}$$

and from (2.20)

$$\limsup_{n\to\infty} P_n^c \le \frac{1}{\frac{1}{W(\phi-1)} + \frac{1}{W}} = \frac{\phi - 1}{\phi} W = \overline{P}^c \tag{2.24}$$

Based on (2.16), a steady state lower bound on P_n^c can be found as

$$\liminf_{n\to\infty} P_n^c \ge \frac{\Gamma - 1}{\Gamma} W = \underline{P} \tag{2.25}$$

Note that $\phi > 1$, so the right hand side of (2.24) is positive.

So, in this case, the upper bound on P_n for EKF will go to a constant value which is determined only by the variance of measurement noise W and ϕ. The upper bound P_n^c also approaches a constant value which is only determined by the variance of measurement noise W and ϕ. This steady state value is less than that of P_n since $\phi > 1$ and also is less than the variance of measurement noise W , which cannot be guaranteed by the EKF.

Type III system with $\phi = 1$:

If $\phi = 1$, then

$$\lim_{n\to\infty} P_n = 0 \tag{2.26}$$

$$\lim_{n\to\infty} P_n^c = 0 \tag{2.27}$$

Note that in this case, though, P_n approaches 0 much slower, at a rate proportional to $\frac{1}{n}$ according to (2.17). Because $P_n > 0$, the transient values of P_n^c will be smaller than P_n and the steady state value of P_n^c will go to zero at a rate proportional to $\frac{1}{n}$ as well.

3. SIMULATION RESULTS

Although types I, II and III systems considered above have been studied in our simulations, only the type II system simulation results will be shown in this section for verification of theoretical results, because all chaotic systems that we have considered are of this type. In this paper, four different first order chaotic maps are investigated.

A. Tent Map

This tent map is defined as

$$x_{n+1} = \begin{cases} a(1-|2x_n - 1|) & 0 \le x_n \le 1 \\ 0 & elsewhere \end{cases}$$

When a is between 0.5 and 1, the trajectory of this map exhibits chaotic behavior. We select $a = 1$, W=1, randomly generating initial value x_0 and $\hat{x}_0$.

In this work, we assume that $f(x)$ is differentiable as many times as needed over its domain of definition as is done in EKF applications. Obviously, this is not true for piecewise linear systems that potentially exhibit chaotic behavior and, therefore, are of interest in chaotic synchronization. However, as we frequently do in practice in applying EKF to non-differentiable nonlinearities, the derivatives will be assigned numerical values at points of discontinuity of the derivatives.

Figure 1 shows the EKF and COO simulation results for variance P_n vs. iteration time n. For EKF, as $n \to \infty$, $P_n \to (\phi - 1)W = 2.24 = \overline{P} = \underline{P}$, where $\overline{P}$ and $\underline{P}$ are defined in (2.23) and (2.25). For COO, as $n \to \infty$, $P_n^c \to \frac{\varphi - 1}{\varphi} W = \overline{P}^c = 0.69$. The theory predicts that the supremum and infimum are the same, giving us the limiting value as are validated for both cases by Figure 1. At the same time, it shows that COO performs better than EKF in the sense of error variance.

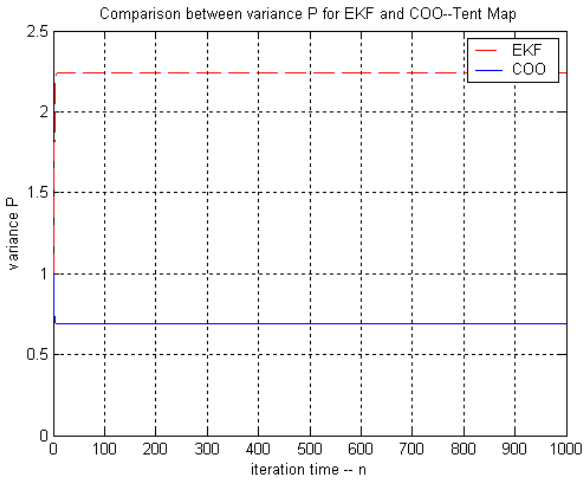

Figure 1. Variance P comparison between EKF and COO vs. iteration time n for type II system-Tent Map

Figure 2 shows the EKF and COO simulation results for sample mean square error vs. iteration time n. The mean square error for EKF is bounded above by 2.24, whereas the mean square error of COO is bounded above by 0.65, which is much smaller than that of EKF. So, COO outperforms EKF also in the sense of sample mean square error.

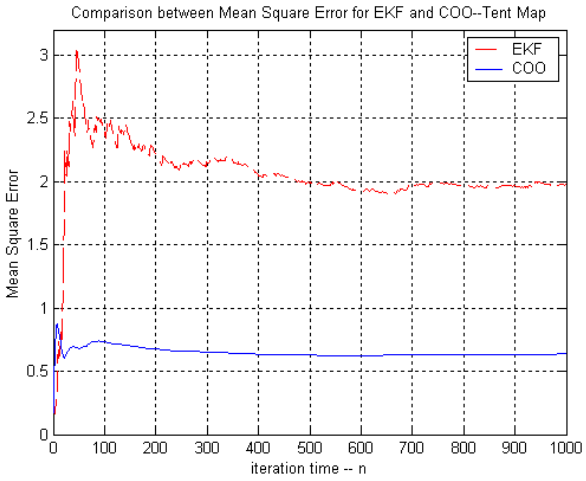

Figure 2. Mean square error comparison between EKF and COO vs. iteration time n of type II system-Tent Map

B. Skew Tent Map

The Skew Tent map is defined (Pecora et al.,1990) by

$$x_{n+1} = \begin{cases} x_n / a, & 0 \le x_n \le a \\ (1 - x_n)/(1 - a), & a < x_n \le 1 \end{cases}$$

In our work, we assign $a = 0.6$, W=1, randomly generate initial value x_0 and $\hat{x}_0$.

Figure 3 shows the EKF and COO simulation results for variance P_n vs iteration time n. For EKF, as $n \to \infty$, P_n is bounded above by $(\phi - 1)W = (1/(1-a))^2 - 1 = 5.25$.

The lower bound of P_n is: $\underline{P} = (1/a)^2 - 1 = 1.78$. For COO, as $n \to \infty$, the upper bound on P_n^c approaches $\frac{\phi - 1}{\phi} W = \frac{(1/(1-a))^2 - 1}{(1/(1-a))^2} * 1 = 0.84.$ The lower bound of P_n^c is: $\underline{P}_n^c = \frac{(1/a)^2 - 1}{(1/a)^2} = 0.64$.

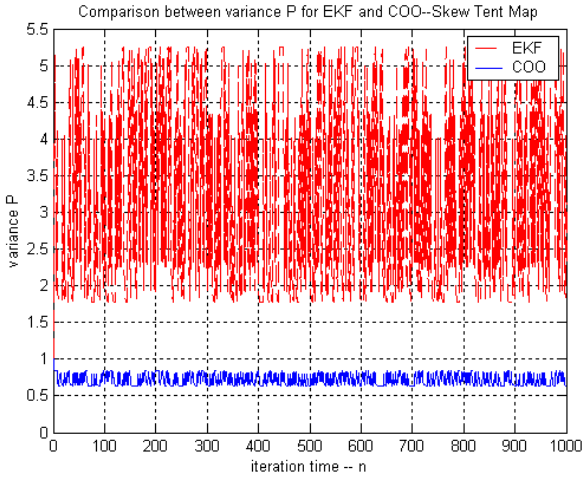

Figure 3. Variance P comparison between EKF and COO vs. iteration time n for type II system-Skew Tent Map

Figure 4 shows the EKF and COO simulation results for sample mean square error vs. iteration time n. For EKF, we can see that the mean square error is bounded above by 3.3. In this case, however, the bound is not tight. For COO, we can see that the mean square error is bounded above by 0.8, which is much smaller than that of EKF.

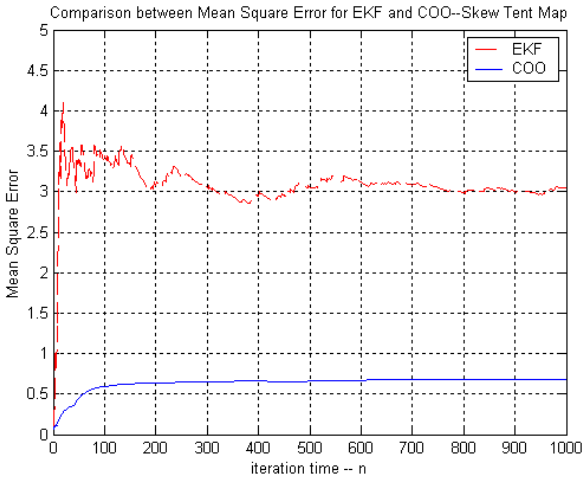

Figure 4. Mean square error comparison between EKF and COO vs. iteration time n of type II system-Skew Tent Map

C. Quadratic Map

The Quadratic map is defined (Devaney, 1989) by

$$x_{n+1} = x_n^2 - a$$

In our work, we assign $a = 2$ for which the orbit exhibits chaotic behavior, W=0.1, and randomly generate initial value x_0 and $\hat{x}_0$.

For variance P_n vs. iteration time n, EKF diverges very fast because the second derivative of quadratic map is not small which is an important assumption of the result in (Zhai, et al., 2003), so we do not include the graph of the variance. However, for COO, although the second derivative is not small and therefore our condition (2.3) is not satisfied, as $n \to \infty$, P_n^c remains bounded and the graph of variance is given in figure 5.

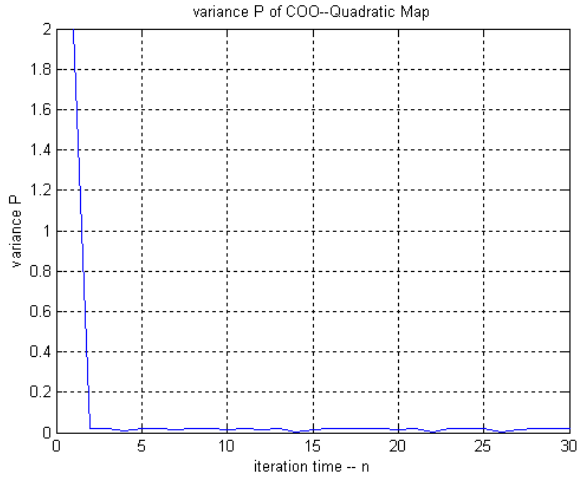

Figure 5. Variance P of COO vs. iteration time n for type II system-Quadratic Map

For sample mean square error vs. iteration time n, EKF diverges very fast because the important assumption in (Zhai, et al., 2003) is not met, so we do not show the graph of mean square error. However, for COO, although again for a large second derivative, we can see that the mean square error is bounded and smaller than the noise variance, which is shown in figure 6.

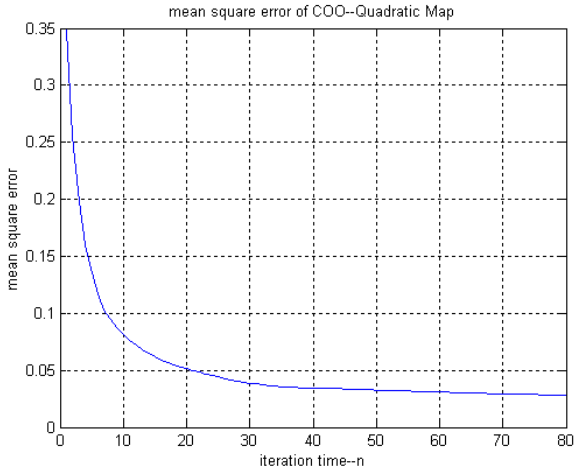

Figure 6. Mean square error of COO vs. iteration time n of type II system-Quadratic Map

D. Cubic Map

The Cubic is defined (Devaney, 1989) by

$$x_{n+1} = ax_n(1-x_n^2)$$

In our work, we assign $a = -2.3$ to have in the chaotic regime, W=0.1, and randomly generate initial value x_0 and $\hat{x}_0$.

For variance P_n vs. iteration time n, EKF, for the same reason given before, diverges very fast, so we do not show its graph. However, for COO, even the second derivative is not small, as $n \to \infty$, P_n^c is bounded and is shown in figure 7.

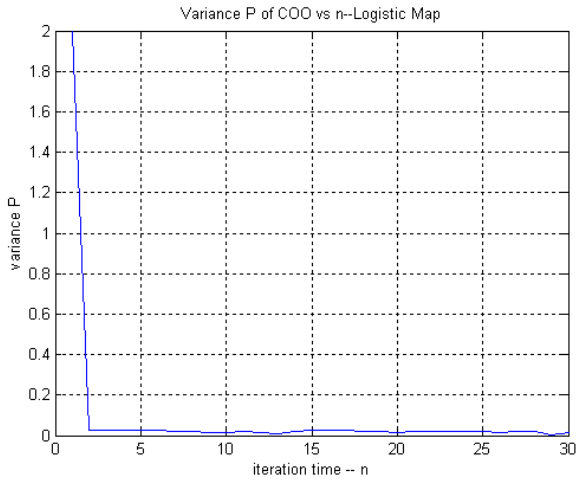

Figure 7. Variance P of COO vs. iteration time n for type II system-Cubic Map

For mean square error vs. iteration time n, EKF again diverges, so that we do not show the graph. However, for COO, we can see that the sample mean square error is bounded and smaller than the noise variance, which is shown in figure 8.

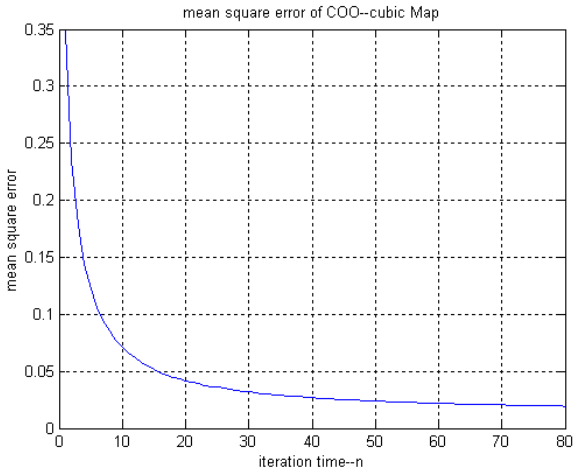

Figure 8. Mean square error of COO vs. iteration time n of type II system-Cubic Map

4. CONCLUSION

A current output type observer is presented in this paper for estimating the state of nonlinear stochastic systems and its performance is evaluated both theoretically and in simulations. It is shown that performance improvement can be obtained by this new scheme over the extended Kalman filter with minor increase in computational load. A categorization of nonlinear systems according to the value of the upper bound on the derivative of the nonlinear function that was formally introduced in (Zhai, et al., 2003) by the authors is considered and comparative performance of the present estimation scheme with respect to EKF is shown. This categorization provides a quantitative method to evaluate the state estimation performance of the new estimator for scalar nonlinear systems, thus potentially facilitating, e.g. the design of chaotic synchronization systems. The simulation results involving state estimation of four different chaotic maps complement the theoretical ones.

REFERENCES

Amirazodi, J. (2001) Nonlinear Observer-Based Synchronization of Chaotic Systems with Application to Secure Communication. Ph.D. Dissertation, University of Arkansas.

Anderson, B. D. O. and J. B. Moore, (1979). Optimal Filtering *Information and system science series*, Prentice Hall, Englewood Cliffs, NJ.

Cruz, C. and H. Nijmeijer. (2000) Synchronization through Filtering. *Int. J. Bifurcation Chaos*, vol. 10, pp. 763-775.

Devaney, R. (1989) *An Introduction to Chaotic Dynamical Systems,* Addison-Wesley, Reading, MA.

Hounkpevi, F. O. and E. E. Yaz (2006a), Third Party Demodulation of a Chaotic Communication Scheme Using Adaptive Estimation via Parallel Processing. *Proceedings of American Control Conference,* Minneapolis, MN, pp. 662-667.

Hounkpevi, F. O. and E. E. Yaz (2006b), An Improved Nonlinear Estimation-Based Chaotic Communication Scheme. *Proceedings of IEEE International Conference on Control Applications,* Munich, Germany, pp. 1426-1431.

Gustafsson, F. (2000). *Adaptive Filtering and Change Detection*, John Wiley & Sons, New York.

Horn, R. A., and C. R. Johnson,. (1991) *Topics in Matrix Analysis,* Cambridge University Press, New York.

Kailath, T., A. H. Sayed, and B. Hassibi (2000) *Linear Estimation, Information and System Sciences Series,* Prentice Hall, Upper Saddle River, NJ.

Leung, H. and Z. Zhu. (2001) Performance Evaluation of EKF-based Chaotic Synchronization, IEEE Trans. *Circuits and Systems-I: Fundamental Theory and Applications,* vol. 48, pp. 1118-1125.

Lewis, F. L. (1986). *Optimal Estimation*, Wiley: New York.

Pecora, L. M. and T. L. Carroll. (1990) Synchronization in Chaotic Systems. *Physical Review Letters,* vol. 64, no. 8, pp. 821-824.

Reif, K., S. Gunther, E. Yaz and R. Unbehauen (1999) Stochastic Stability of the EKF: the Discrete-Time Case, *IEEE Trans. Autom. Contr.*, vol.44, pp. 714-728.

Ruan, H., T. Zhai and E. Yaz. (2003a) A Demodulation Scheme Based on State Estimation for Chaotic Digital Communication. *Proceedings of 2003 American Control Conference,* Denver, CO, pp. 1614-1618.

Ruan, H., T. Zhai and E. Yaz. (2003b) A Chaotic Secure Communication Scheme with Extended Kalman Filter Based Parameter Estimation. *Proceedings of IEEE International Conference on Control Applications,* Istanbul, Turkey, pp. 404-408.

Sobiski, D. J. and J. S. Thorp. (1998) PDMA-1: Chaotic Communication via the Extended Kalman Filter. *IEEE Trans. Circuits Systems,* vol. 44, pp.194-197.

Zhai, T., H. Ruan, E. E. Yaz, and Y.I. Yaz. (2003) Performance Evaluation of Extended Kalman Filter Based State Estimation for first Order Nonlinear Dynamic Systems, *Proceedings of IEEE Conference on Decision and Control,* Hawaii, pp. 1386-139.